Atmospheric Environment 290 (2022) 119355

Contents lists available at ScienceDirect

Atmospheric Environment

journal homepage: www.elsevier.com/locate/atmosenv

Strong ozone intrusions associated with super dust storms in East Asia

Yu Yang [a,b], Zilin Wang [a,b,**], Sijia Lou [a,b,c], Lian Xue [a,b,c], Jinpeng Lu [a,b], Hongyue Wang [a], Jiandong Wang [d], Aijun Ding [a,b,c], Xin Huang [a,b,c,*]

[a] School of Atmospheric Sciences, Nanjing University, Nanjing, China
[b] Jiangsu Provincial Collaborative Innovation Center for Climate Change, Nanjing, China
[c] Frontiers Science Center for Critical Earth Material Cycling, Nanjing University, Nanjing, China
[d] Key Laboratory for Aerosol-Cloud-Precipitation of China Meteorological Administration, School of Atmospheric Physics, Nanjing University of Information Science and Technology, Nanjing, China

HIGHLIGHTS

- A rapid increase in nighttime ozone near the surface is observed during the strong dust storm in March 2021.
- The synoptic system associated with the dust storm is also conducive to Stratosphere-Troposphere Exchange.
- Asian dust storm is often accompanied by surface ozone anomaly due to stratospheric ozone intrusion.

ARTICLE INFO

Keywords:
Spring dust
Ozone
Stratospheric intrusion
East asia
Vertical exchange

ABSTRACT

As one of the largest dust source regions, China suffers from frequent dust storms in spring. During the super dust storm in March 2021, a rapid increase in nocturnal surface ozone concentration was observed along with elevated dust loading. Ground-based and satellite observations as well as reanalysis data of air quality and meteorology are integrated to shed light on the ozone anomaly. It is indicated that cold fronts and cyclones are conducive to both dust emissions and the downwards transport of stratospheric air, leading to simultaneously soaring ozone and particle concentrations near the surface. Statistically, in the past few years, under the influence of specific synoptic weather accompanied with Stratosphere-Troposphere Exchange (STE), dust was frequently uplifted to 8–12 km and the low-tropospheric ozone was elevated by approximately 6 ppb in northern China during spring dust storms. This work reveals strong ozone intrusions associated with dust storms, which have great impacts on atmospheric chemistry and regional climate.

1. Introduction

As an important component of atmospheric aerosols, mineral dust accounts for more than half of the mass loading of global aerosols (Textor et al., 2006; Zender et al., 2004). After emission, dust can deteriorate local and regional air quality and exert an adverse impact on public health (Duce et al., 1980; Eguchi et al., 2009; Lee et al., 2007; Shiraiwa et al., 2017). Dust aerosols can also function as an external source of nutrients and trace elements when depositing into the ocean, affecting the ocean biogeochemistry cycle (Jickells et al., 2005; Mahowald et al., 2005; Ren et al., 2011). By interacting directly with radiation and indirectly with clouds, dust aerosols could exert a substantial impact on regional and global climate (Choobari et al., 2014). On the one hand, dust aerosols can significantly influence cloud microphysics by serving as cloud condensation nuclei or ice nuclei (Kaufman et al., 2005; Su et al., 2008). On the other hand, aerosols play a key role in radiation transfer and atmospheric temperature perturbation (X. Huang and Ding, 2021). As absorbing aerosols, dust has been proven to absorb and scatter both short- and long-wave radiation, resulting in cooling near the surface and warming in the upper layer (J. Huang et al., 2014; L. Liu et al., 2016; W. Wang et al., 2013; Z. Wang et al., 2018). Such modifications in temperature stratification would stabilize the boundary layer and further suppress the diffusion of near-surface pollutants (Wang et al., 2020; Yang et al., 2021).

* Corresponding author. School of Atmospheric Sciences, Nanjing University, Nanjing, China.
** Corresponding author. School of Atmospheric Sciences, Nanjing University, Nanjing, China.
E-mail addresses: zilinwang@smail.nju.edu.cn (Z. Wang), xinhuang@nju.edu.cn (X. Huang).

https://doi.org/10.1016/j.atmosenv.2022.119355
Received 8 March 2022; Received in revised form 8 August 2022; Accepted 20 August 2022
Available online 27 August 2022

Dust storms mainly originate from arid and semi-arid desert regions (Zhang et al., 2003). As one of the largest dust source regions across the world, East Asia features frequent spring dust storms, which are related to cold fronts and cyclones in spring (Husar et al., 2001; W. Li et al., 2018; Qian et al., 2002; Sun and Zhao, 2008; L. Zhao & S. Zhao, 2006). Asian dust mainly sources from the Taklimakan and Gobi Deserts in the north and northwest of China (Choobari et al., 2014; Prospero et al., 2002), and can be transported to southeast regions and even across the Pacific Ocean (Husar et al., 2001; In and Park, 2002; Takemura et al., 2002). Synoptic systems can significantly influence the vertical transport and distribution of mineral particles. Tsai et al. (2008) indicated that dust particles in the front of an upper level trough could be uplifted into the free troposphere while dust particles behind the trough generally remained in the lower troposphere below 700 hPa. Several existing studies have pointed out that the upward motion of air mass associated with cyclones could uplift the dust particles to the upper troposphere (Cuesta et al., 2015; M. Liu et al., 2003). The uplifted dust near the source regions was transported downwind and then subsided to the earth surface, causing particulate pollution in the downwind areas especially eastern China (F. Wang et al., 2021; Wei et al., 2018). Dust storms have various and wide-ranging negative impacts on society. Through worsening air quality, dust storm events usually result in increased rates of morbidity and mortality for cardiovascular and respiratory diseases (Aili and Kim Oanh, 2015; Goudarzi et al., 2017; Khaniabadi et al., 2017). The adverse effects of dust storms on the economy can also be severe. The accidents, cancellations, and delays in road, rail, and air transportation systems due to dust storms lead to substantial economic losses (AlKheder and AlKandari, 2020; Middleton et al., 2019; Miri and Middleton, 2022). Moreover, dust storms also cause damage to agriculture by weakening soil stability and severely affecting photosynthesis (Al-Hemoud et al., 2017; Mohamed and Gehan, 2012). The electricity and solar power generation are seriously affected as well (Gholami et al., 2018; Pahlavanravi et al., 2012), with buildings and infrastructures destructed by strong winds (Miri et al., 2009).

In the mid- and high-latitudes of the northern hemisphere, Stratosphere-Troposphere Exchange (STE) occurs frequently in spring due to specific synoptic systems (Lelieveld and Dentener, 2000; Liang et al., 2011; Škerlak et al., 2014). As an important dynamic process, it changes the oxidative capacity of the troposphere and potentially affects the climate system (Holton et al., 1995). Previous works have shown that the occurrence of STE is usually associated with cyclones, fronts, the Brewer-Dobson circulation, tropopause folding, Rossby wave breaking, moist convection, and cut-off lows (Dimitris Akritidis et al., 2018; Holton et al., 1995; Krasauskas et al., 2021; D. Li et al., 2015; Salby and Callaghan, 2006). Mid-latitude cyclones enable the vertical transport of O_3 from the lower stratosphere into the troposphere (K. Emma Knowland et al., 2017; Sprenger, 2003). Moreover, tropopause folds are the main mechanism of stratosphere-to-troposphere transport (STT) events (Stohl, 2003) and lead to the downward transport of stratospheric O_3-rich air into the troposphere (Danielsen and Mohnen, 1977), which is defined as stratospheric intrusion (SI). Therefore, SI is considered to be one of the important processes that contribute to tropospheric ozone (A. Ding & T. Wang, 2006; Mkololo et al., 2020). Occasionally, stratospheric O_3-rich air is transported deep down to the lower troposphere or even the ground, resulting in surface ozone pollution (D. Akritidis et al., 2010; Knowland et al., 2017; Lefohn et al., 2011; Lin et al., 2012).

Dust storms and stratospheric ozone intrusion both frequently occur during spring in East Asia, with drastic change of surface PM_{10} and O_3 recorded (Kim et al., 2002; Takemi, 2005; Tan et al., 2012). However, few studies have focused the joint variations of such two important atmospheric compositions and explored the inherent relations in between. In this study, we analyzed the influence of synoptic systems on the vertical transport of dust particles and O_3 based on a strong dust storm in 2021 with intensive STE. A strong dust storm hit northern China on March 15th, 2021, the air quality in northern China was deteriorated, with the average PM_{10} concentration in the early morning of the storm day above 3000 μg/m^3. Notably, this event was accompanied by the anomalous nocturnal O_3 increase near the surface in northern China. Here, by combining real-time observations and reanalysis data, we investigate the synoptic causes of stratospheric O_3 intrusion during this extreme dust storm event. Furthermore, statistical analysis of long-term satellite retrievals and surface observation data indicate that the vertical exchange of atmospheric compositions during strong dust storm is frequently occurred, exerting great impact on atmospheric chemistry and regional climate. The rest of this article is structured as follows. The datasets used in this work are introduced in Section 2. Then, Section 3 contains the overview of the super dust storm and ozone pollution as well as the long-term analysis of their joint variations. The impact of the synoptic systems on vertical exchange of the dust particles and O_3 is also included. Conclusions are summarized in Section 4.

2. Datasets

2.1. Observational data

2.1.1. Pollutant and meteorological observation

Ground-based pollutants concentration such as $PM_{2.5}$, PM_{10}, O_3 at more than 1500 stations are openly available from the air monitoring data center of the Ministry of Ecology and Environment of People's Republic of China. Such observational dataset with an hourly temporal resolution covers most parts of China and provides a comprehensive vision of air quality in China. Numerous existing studies have used this dataset to analyze the spatial and temporal variations of air pollution events (X. Huang et al., 2018; Z. Wang et al., 2020). In this study, this dataset was applied to analyze the evolution of particulate matter and O_3 during the dust storm events.

The hourly ground-based meteorological condition datasets, including horizontal visibility and wind speed and direction etc., archived at the US National Climate Data Center (NCDC) were collected to identify the dust storm as well as analyze the synoptic causes of the strong vertical exchange of dust particles and O_3. The horizontal visibility and the near-surface wind speed are often applied to identify and classify dust storms (Cao et al., 2018; S. Wang et al., 2005), and thus we used them to select strong dust storm days during the spring of 2013–2020. In various previous works, the definition of dust storms showed some disparities. For strong dust storms in Asia that were concerned in the study, Indoitu et al. (2012) defined it as wind speeds reaching 10–14 m/s with the horizontal visibility lower than 1000 m. An et al. (2018) defined a sand and dust storm event in Asia as at least three standard stations recorded wind speeds greater than 3 m/s with the horizontal visibility less than 1000 m. Since the regions we focused on were located in northern China and southern Mongolia with little anthropogenic activity, the horizontal visibility was mainly affected by natural pollution sources such as dust aerosols rather than anthropogenic pollution sources. Meanwhile, the generally assumed threshold wind speed of Asian dust suspension was 9 m/s (Kurosaki and Mikami, 2007). Consequently, based on the above researches, we defined the strong dust storms days as at least three standard ground stations of northern China and southern Mongolia recorded the near-surface wind speed greater than 10 m/s and the horizontal visibility less than 1000 m on the same day. For the radiosonde data, water vapor mixing ratio and potential temperature profiles are measured twice a day (00:00 and 12:00 UTC) on primarily mandatory pressure levels, which are employed to provide direct signal on vertical stratification.

2.1.2. Satellite observations

The Moderate resolution Imaging Spectroradiometer (MODIS) Aqua satellite data were adopted in this study, which passed the study region at 13:30 local time (LT) on March 15–16th, 2021. MODIS Level 2 Deep Blue products of aerosols optical depth (AOD) at 550 nm with a horizontal resolution of 10 km (MYD04) were collected to show the spatial distribution and the evolution of the dust aerosols. Spatio-temporal

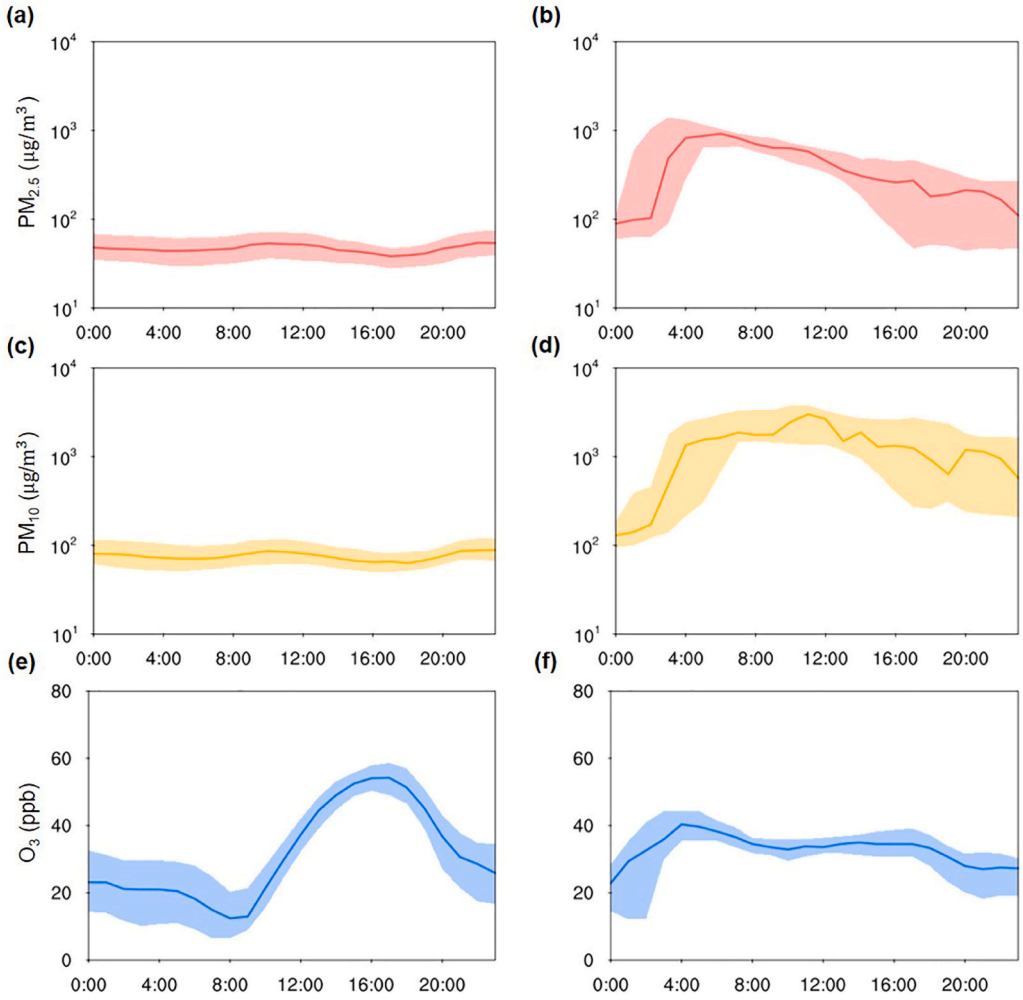

Fig. 1. Diurnal variations of (a, b) $PM_{2.5}$, (c, d) PM_{10}, and (e, f) O_3 before the dust episode (Column1, average from March 9–14th, 2021) and on the day of the dust outburst (Column2, March 15th, 2021) in northern China.

variations in the AOD using MODIS data had been widely employed to study the dust storm events (Alam et al., 2014; Kaskaoutis et al., 2008). Meanwhile, the Cloud-Aerosol Lidar and Infrared Pathfinder Satellite Observations (CALIPSO version 4) satellite were also used. Data from CALIPSO Level 2 Vertical Feature Mask (VFM) was adopted to analyze the vertical distribution and transport of dust aerosols during dust storms (Jose et al., 2016; Tan et al., 2017).

2.2. Reanalysis data

2.2.1. CAMS global reanalysis data

The CAMS global reanalysis is the latest ECMWF (European Centre for Medium-Range Weather Forecasts) global reanalysis of atmospheric compositions for the period from 2003 onward. It was produced using four-dimensional variation assimilation (4D-Var) in CY42R1 of ECMWF's Integrated Forecast System (IFS) (Inness et al., 2019). The chemical mechanism of the IFS is an extended version of the Carbon Bond 2005 (CB05) mechanism, which contains tropospheric chemistry with 126 reactions (Flemming et al., 2015). Stratospheric ozone chemistry in IFS is parameterized by the Cariolle scheme (Cariolle and Déqué, 1986; Cariolle and Teyssedre, 2007). Previous studies have shown that such a combination makes a good representation of realistic tropospheric and stratospheric O_3 concentrations (Huijnen et al., 2020; Inness et al., 2019). In addition, CAMS reanalysis verification reports (https://atmosphere.copernicus.eu/eqa-reports-global-services) indicate that the stratospheric O_3 in the CAMS reanalysis is within ±5–10% consistent with ozonesondes and satellite observations and does not show any significant bias trends. Apart from O_3, stratospheric ozone tracer (O_3S) is also provided in CAMS, which is defined as ozone mixing ratios in the stratosphere and is only subject to chemical loss and deposition in the troposphere. The only source of O_3S in the troposphere is the influx from the stratosphere. Some previous studies have used the O_3S in CAMS to analyze the ozone variability in the atmosphere (Dimitris Akritidis et al., 2021). Therefore, O_3S applied in this study can reasonably respresent stratospheric O_3 entering the troposphere with limited uncertainties. The CAMS reanalysis has a spatial resolution of approximately 80 km (0.75° × 0.75° grid) with 60 hybrid sigma-pressure (model) levels up to 0.1 hPa, and a temporal resolution of 3 h.

2.2.2. ERA5 reanalysis data

ERA5 is the fifth generation ECMWF reanalysis for the global climate and weather with a spatial resolution of 0.25° × 0.25° and a temporal resolution of 1 h (Hoffmann et al., 2019). The ERA5 dataset can be well used to analyze the synoptic weather in East Asia (L. Zhao et al., 2020). The geopotential height at 925 hPa and 500 hPa, vertical velocity (ω) at 500 hPa, and wind fields provided by the ERA5 dataset were collected to study the synoptic conditions during the dust storms. In addition, potential vorticity (PV) was provided by the ERA5 dataset to display the spatial and temporal changes of PV during the event.

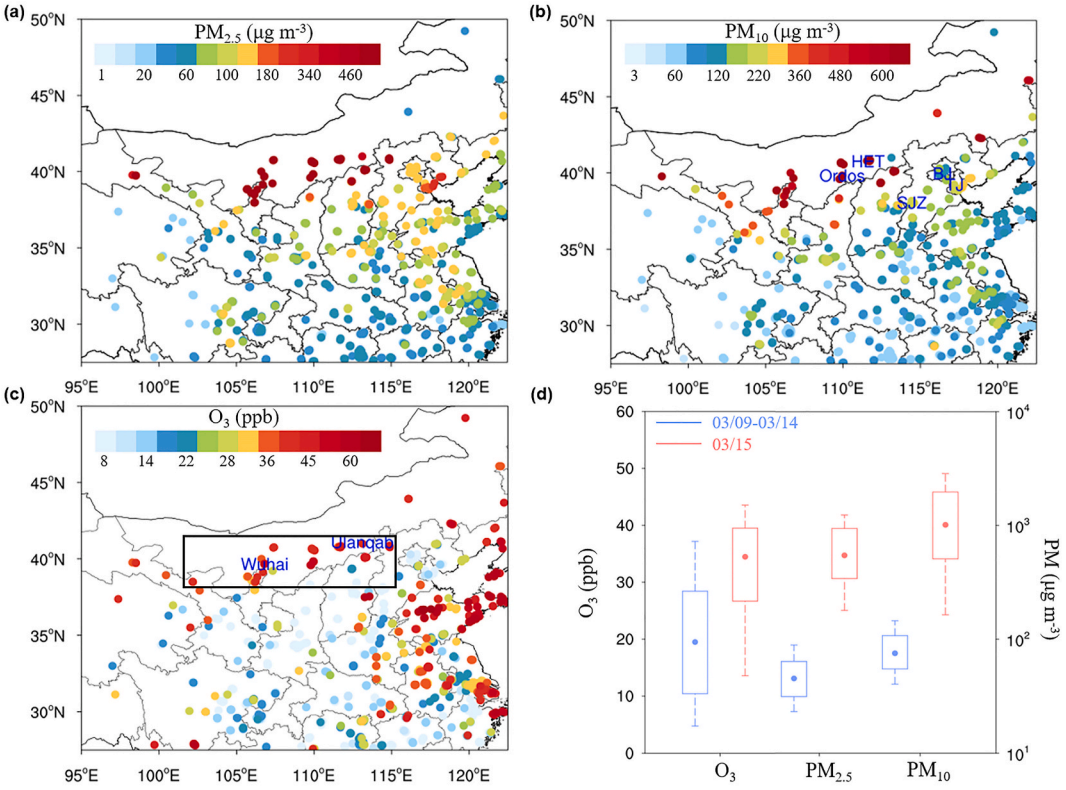

Fig. 2. Spatial distribution of (a)$PM_{2.5}$, (b)PM_{10}, and (c)O_3 at 06:00 LT on March 15th, 2021 recorded by air quality monitoring stations. (d) O_3, $PM_{2.5}$, and PM_{10} concentrations in the early morning (00:00LT-08:00LT) before the dust episode (blue; the average from March 9–14th, 2021) and on the dust outburst day (red; March 15th, 2021). Note that the dots in the boxes represent the average values, the boxes and whiskers represent the 10th, 25th, 75th, and 90th percentiles respectively. The stations enclosed by the black rectangle in (c) have been selected to perform analysis for the comparision in (d). (For interpretation of the references to colour in this figure legend, the reader is referred to the Web version of this article.)

3. Result

3.1. The overview of the super dust storm

The outbreak of the super dust episode in March 2021 was associated with the development and movement of the Mongolian cyclone. The high wind speeds resulting from the Mongolian cyclone usually tend to promote dust emissions from the Gobi Desert (J.-T. Liu et al., 2004; M. Liu et al., 2003). On March 14th, 2021 the Mongolian cyclone over eastern Mongolia followed by high-pressure system led to strong westerly winds over the Gobi Desert due to an intense pressure gradient (Fig. S1b). The strong westerly wind speeds over the Gobi exceeded the generally assumed dust-generating wind speeds threshold of Asia (Kurosaki and Mikami, 2007), reaching over 20 m/s. Furthermore, according to statistical results based on reanalysis data in the past decade, the intense surface evaporation caused by warming air temperature (Fig. S2) and deficient precipitation (Yin et al., 2021) led to a low relative humidity in early March 2021 (Fig. S3). The lack of moisture accelerated soil drying near dust sources and was conducive to dust emissions. Therefore, combined with the strong westerly winds and the low relative humidity near the dust sources, the dust storm broke out in Mongolia on March 14th, 2021. On the second day, the Mongolian cyclone moved eastward to northeast China followed by a high-pressure center over Mongolia, which resulted in northwesterly airflow between the low-pressure and high-pressure centers (Fig. S1c). The northwesterly wind promoted the transport of dust aerosols from the source regions to Inner Mongolia. Consequently, the super dust storm affected northern China from the early morning of March 15th and swept over the downwind areas.

According to the air quality monitoring stations in northern China, under the influence of the strong dust storm, the concentrations of particulate matter increased sharply from the early morning of March 15th with the average PM_{10} concentration exceeding 1000 $\mu g/m^3$ (Fig. 1d). Furthermore, both the PM_{10} and $PM_{2.5}$ concentrations were greatly enhanced on the dusty day compared to those before the dust storm in northern China (Fig. 2d). Located close to the dust source region, Ordos and Hohhot witnessed the maximum hourly PM_{10} concentration reached as high as 9985 $\mu g/m^3$. As the dust plume moved eastwardly, the Beijing-Tianjin-Hebei region was also greatly affected by the super dust storm with maximum hourly PM_{10} concentration reaching 9753 $\mu g/m^3$ at Beijing, 3205 $\mu g/m^3$ at Shijiazhuang, and 2199 $\mu g/m^3$ at Tianjin. Such high particle concentrations not only caused serious deterioration of air quality, but also had substantial adverse effects on atmospheric visibility. In Mongolia the severe dust storm was reported to cause six deaths and left dozens missing, and hundreds of flights were cancelled or grounded at Beijing airports as the horizontal visibility in most of storm-affected areas was less than 1 km (https://www.bbc.com/news/av/world-asia-china-56399268). Moreover, high AOD values of more than 1.5 were captured by MODIS from Inner Mongolia to Beijing-Tianjin-Hebei regions on March 15th, 2021, which exhibited a good correspondence with the spatial PM_{10} distribution (Figs. 2b and 3a). In addition, the high AOD regions were accompanied by high absorbing AOD (AAOD in Fig. 3c), indicating the great influence from light-absorbing dust aerosols. At the same time, the near-surface O_3 concentration in northern China was also abnormally higher compared to that before the dust episode (Fig. 1e and f, Fig. 2d). The near-surface O_3 concentration had a significant diurnal variation and reached the diurnal peak at about 16:00LT before the episode (Fig. 1e). However, during the dust storm, the diurnal variation of the near-surface O_3 concentration disappeared and the highest concentration was detected at 04:00LT (Fig. 1f). Such an abnormal ozone peak during the nighttime would be further discussed in chapter 3.2. On March 16th, 2021, as the

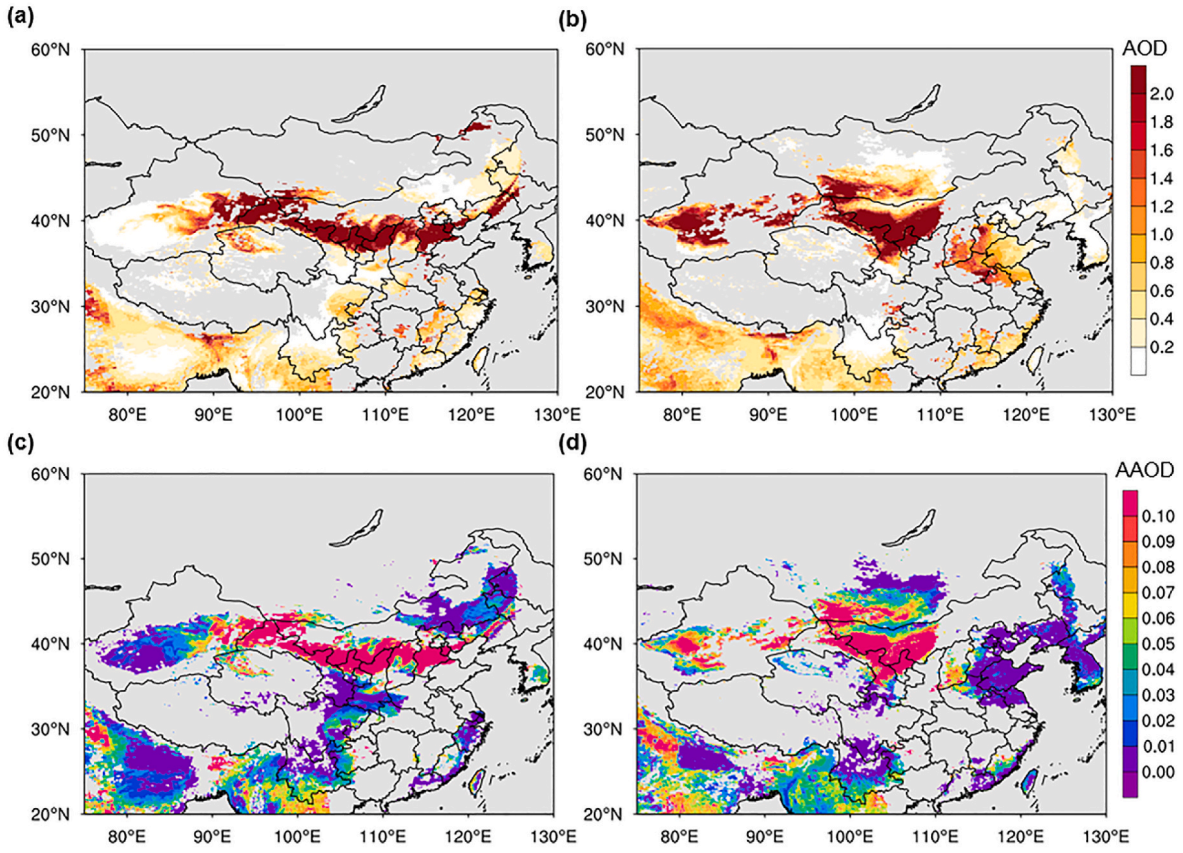

Fig. 3. (a, b) Aerosol optical depth (AOD) and (c, d) absorbing aerosol optical depth (AAOD, derived from AOD*(1-SSA)) at 550 nm over eastern Asia retrieved by MODIS satellite on March (a, c) 15th and (b, d) 16th, 2021. Missing values are shaded in grey.

Mongolian cyclone continued to move eastward (Fig. S1d), the dust plume was transported to eastern China including Shangdong and Henan, where the AOD value exceeded 1.0 (Fig. 3b).

3.2. *Synoptic weather triggering vertical exchange of dust aerosols and ozone*

The upper-level trough related to the Mongolian cyclone constantly developed and moved easterly during the super dust storm (Fig. 4a and b). The center of the shallow trough was located in Mongolia at 14:00LT on March 14th' 2021 and moved to the border between eastern Mongolia and northeast China at 02:00LT on the next day, when the shallow trough developed into a deep trough. According to air mass vertical movement (ω) at 500 hPa, the upward motion of air with vertical velocity of about −0.5 Pa/s existed in the east of the trough (Fig. 4a and b). Therefore, as the trough developed, the ascending airflow in the east of the trough could lift dust particles to the mid troposphere (Fig. 5a and b). In order to better understand the vertical transport of dust particles, the vertical distribution of the dust plume captured by CALIPSO on March 15th with its corresponding track was shown in Fig. 6. The dust plume in the dust source region and nearby areas could be elevated to about 8–12 km (Fig. 6a). The uplifted dust plume prone to long-range transport could exert a critical impact on atmospheric radiation transfer (J. Huang et al., 2008; Zhu et al., 2007).

Contrary to the ascending airflow in the east of the trough, the descending airflow dominated in the west of the trough. Some previous works have suggested that the downward motion behind the trough could lead to the SI during the development and movement of the trough (H. Wang et al., 2020; Y. Wang et al., 2020). The stratosphere has high static stability and contains a larger potential vorticity (PV) compared with the troposphere. Hence, PV could be used as an indicator to distinguish stratospheric air masses from tropospheric ones, which is a common approach to identify STE processes (Kumar et al., 2020; Luo et al., 2013; Zhang et al., 2021). The dynamical tropopause is commonly defined using a PV value of ±2 PVU (1PVU = 10^{-6} K·m^2·s^{-1}·kg^{-1}) (Cui et al., 2004; Holton et al., 1995; Newell et al., 1997). The spatial distribution of PV at 300 hPa was shown in Fig. 4c and d. Abnormally high PV values at 300 hPa could be identified in northern Mongolia at 14:00LT on March 14th, which corresponded to the center of the upper-level trough. Along with the trough development, the broader region with high PV values could be seen over eastern Mongolia and Inner Mongolia. It is suggested that the SI occurred simultaneously with the downward motion behind the trough. In addition, the stratospheric air mass is not only characterized by high PV but also by high O_3, low water vapor and high potential temperature (PT). Thus, the high PV values at 300 hPa indicate that O_3-rich, high-PT, and dry stratospheric air were transported to the troposphere. To illustrate the SI clearly, the spatial pattern of O_3 at 300 hPa was analyzed (Fig. 7). The spatial distribution of high-O_3 at 300 hPa was very similar to that of high-PV, confirming that the O_3-rich stratospheric air was injected into the upper troposphere due to the SI. To better illustrate the downward transport of stratospheric ozone into the troposphere during the development of the trough, the evolution of O_3S was adopted (Fig. 5c and d). As shown in Fig. 5c and d, SI could contribute an increase of 15 ppb to near-surface O_3 concentration at most. According to the vertical profile, the water vapor mixing ratio (mass of water vapor/dry air mass) would sharply drop (Seguel et al., 2018) and potential temperature would increase near the tropopause due to SI (Fig. 8). Under the influence of the SI, water vapor mixing ratio at Ulann-Baator at 12:00UTC on March 14th drastically decreased to 0.01 g/kg at about 500 hPa, much lower than 0.06 g/kg at 00:00UTC on March 15th and the potential temperature increased significantly near the tropopause (Fig. S4 and Fig. 8).

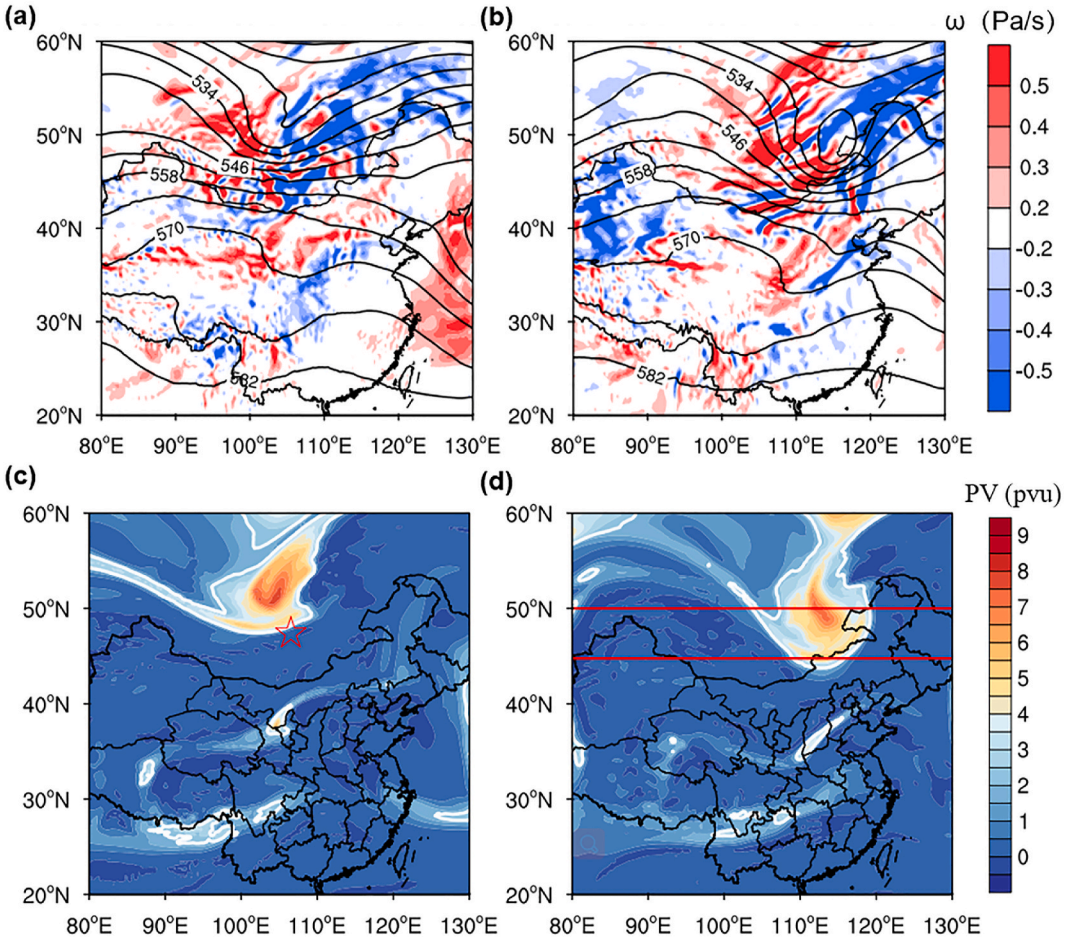

Fig. 4. (a, b) The geopotential height field (the black line, units:dagpm) and vertical velocity (ω) at 500 hPa. (c, d) Spatial distribution of potential vorticity (PV) at 300 hPa. The white contour line corresponds to 2 PVU (1PVU = 10^{-6} K·m^2·s^{-1}·kg^{-1}). Note that the red star in (c) is the Ulaan-Baator, and the latitude ranges of red lines in (d) is the average regions of the cross-section in Fig. 5. Column1 is 14:00LT on March 14th, and column2 is 02:00LT on March 15th. (For interpretation of the references to colour in this figure legend, the reader is referred to the Web version of this article.)

Furthermore, the stratospheric O_3 entering the upper troposphere could be kept for a relatively long time (Young et al., 2013) and further transported to the lower troposphere associated with downward motions of air behind the trough during the dust storm. Such a process could raise the O_3 concentration near the surface far beyond its counterpart during normal days. Coincidentally, a soaring nocturnal ozone was observed in northern China during the super dust storm (Fig. 2c). The hourly concentration at many air quality monitoring stations of northern China could exceed 40 ppb from 04:00 LT on March 15th, much higher than the average O_3 concentration of 21 ppb in the early morning before the super dust storm. The maximum value of hourly O_3 concentration at Wuhai and Ulanqab both reached 50 ppb in the early morning of the dust storm day. Simultaneously, the humidity in troposphere near the dust sources decreased significantly (Fig. S5), suggesting the intrusion of stratospheric dry air. Due to the absence of incident solar radiation at night, the contribution of photochemical reactions to O_3 was expected to be insignificant. Given the negligible role of photochemical production and the simultaneous low tropospheric humidity, the rapid increase in the nocturnal near-surface ozone might be linked to SI. Therefore, the intensive weather system associated with dust storms may significantly affect the transport or diffusion of the atmospheric compositions like dust particles and ozone.

3.3. *Long-term evidence on intensified vertical exchange of O_3 and particles during dust storms*

The aforementioned strong vertical transport of ozone and particles during the dust storm is not occasional. Instead, such processes influenced by similar synoptic conditions frequently occurred over northern China during the past few years based on the comprehensive analysis of the vertical structure of pollutants. As shown in Fig. 9, we compared the surface O_3 concentration and the frequency of positive surface O_3 anomaly on dust storm days and non-dust storm days in the spring of 2013–2020 in northern China. On dust storm days, not only the particle concentration but also the surface O_3 concentration is higher than that on non-dust storm days (Fig. 9a). We also found that positive surface O_3 anomaly frequency was 43% on non-dust storm days but 60% on dust storm days (Fig. 9b). In addition, CAMS reanalysis showed that stratospheric O_3 was transported downward and dust particles were uplifted upward during dust storms (Fig. 10c and d).

Long-term average meteorological conditions of strong dust storm events and spring climatology were displayed in Fig. 10 and Fig. S6, respectively. Compared with the spring climatology, the stronger low-pressure center was located over Mongolia and Inner Mongolia during the dust storms because the dust storms in Mongolia in spring were often caused by cyclones and cold fronts (Husar et al., 2001; Qian et al., 2002). The high-pressure anomaly in the west accompanied with the low-pressure anomaly in the east during the dust storms resulted in westerly airflow anomalies in between (Fig. 10a). As shown in Figs. S6a

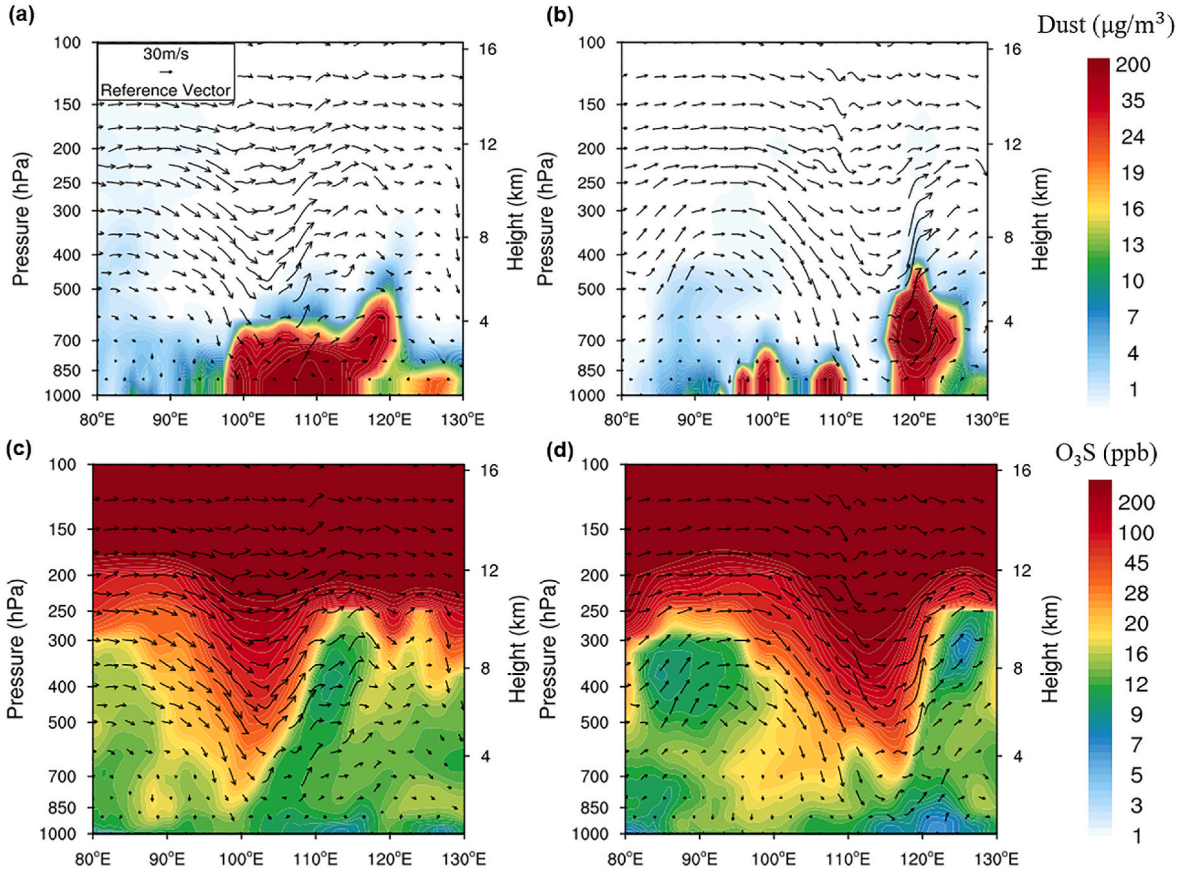

Fig. 5. Longitude-height cross-section (averaged over the latitude regions of red lines in Fig. 4d) of (a, b) dust, (c, d) stratospheric O_3 tracer (O_3S), in-plane wind vectors (arrows) where the vertical speed was multiplied by a factor of 600. (a) and (c) is 14:00LT on March 14th, 2021, and (b) and (d) is 02:00LT on March 15th, 2021. Dust and O_3S are CAMS reanalysis data. (For interpretation of the references to colour in this figure legend, the reader is referred to the Web version of this article.)

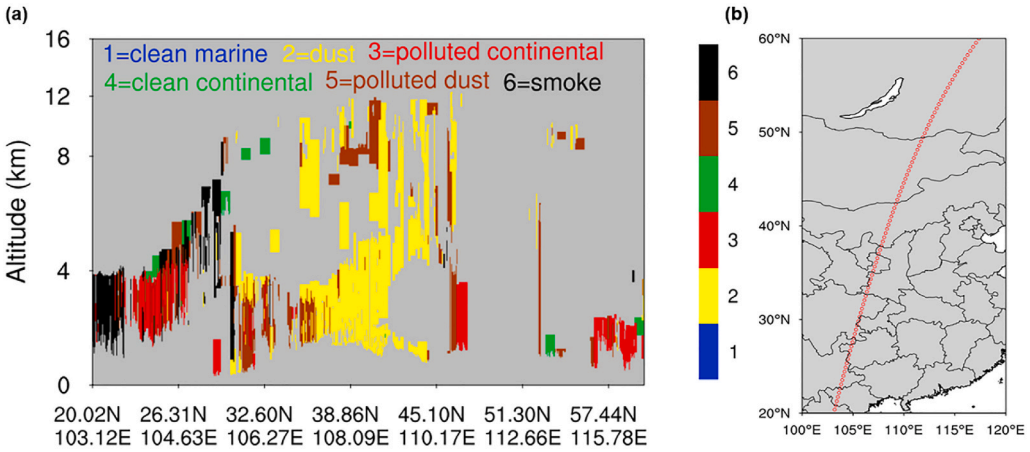

Fig. 6. (a) Vertical cross-section of aerosol types detected by CALIPSO on March 15th, 2021. And (b) the corresponding CALIPSO track.

and S6b, the westerly airflow frequently over dust sources intensified wind speeds during the spring, resulting in the outbreak of dust storms. In addition, the strong ascending airflow anomalies were found over the stronger low-pressure center during the dust storms (Fig. 10b). Due to such upward motions, dust particles could be uplifted to the upper troposphere, which caused the average dust aerosols concentration at 400 hPa to reach 10 μg/m^3 in the downstream areas of dust sources (110°E–120°E) (Fig. 10c). According to the statistical results of CALIPSO data over Inner Mongolia, dust particles were usually concentrated below 4 km but the probability of dust plumes being transported to 8–12 km could also reach about 50% (Fig. S7).

Descending airflow anomalies and positive PV anomalies are indicative of SI behind low-pressure anomalies (Fig. 10b). Therefore, O_3-rich stratospheric air would be transported deep down into the troposphere as the SI developed, leading to a high anomaly O_3 of 6 ppb near the surface over the source region during spring dust storms in the past few years. This phenomenon indicated that the strong dust storm events in spring could be accompanied by O_3 pollution caused by STE process. As

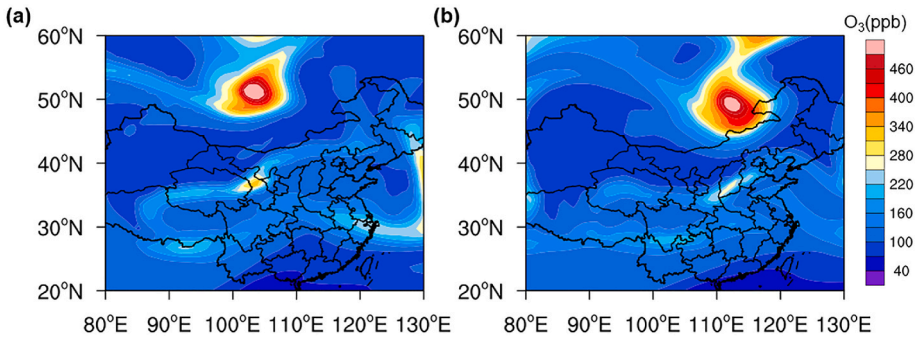

Fig. 7. Spatial distribution of O_3 at 300 hPa at (a) 14:00 LT on March 14th, 2021 and (b) 02:00 LT on March 15th, 2021. O_3 is the result of CAMS reanalysis data.

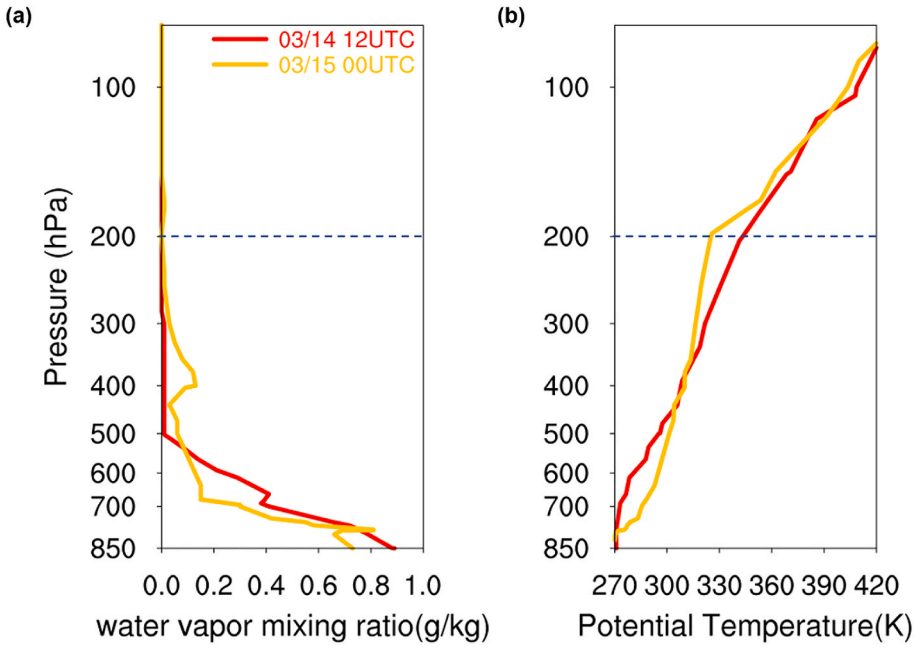

Fig. 8. Vertical profile of (a) water vapor mixing ratio and (b) potential temperature detected by radiosonde observations at Ulaan-Baator (Located at the red star in Fig. 4c; 47.55°N, 106.52°E, 1306 m a.s.l.) at 12:00UTC on March 14th, 2021 and 00:00UTC on March 15th, 2021. The dashed blue line represents the tropopause. (For interpretation of the references to colour in this figure legend, the reader is referred to the Web version of this article.)

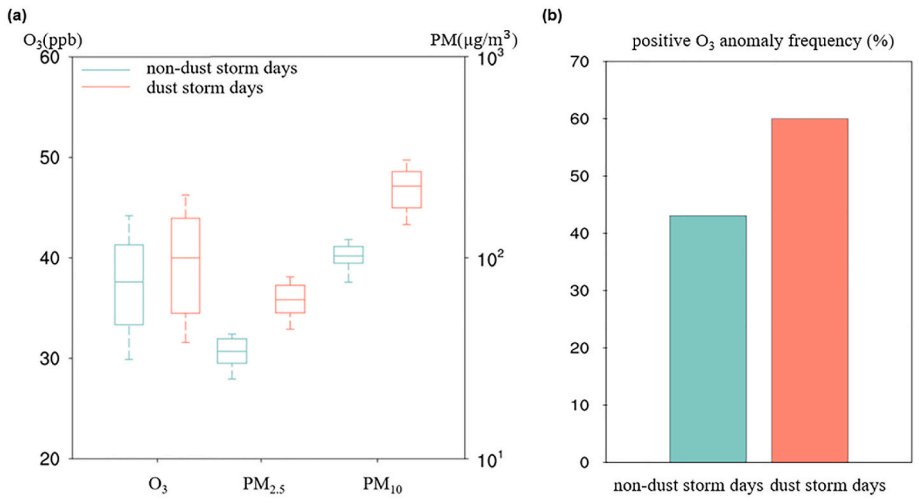

Fig. 9. (a) O_3, $PM_{2.5}$, and PM_{10} concentrations on dust storm days (red) and non-dust storm days (green) in spring from 2013 to 2020 in northern China. Note that horizontal lines in the box present the average values, the boxes and whiskers represent the 10th, 25th, 75th, and 90th percentiles respectively. (b) O_3 positive anomaly frequency on dust storm days (red) and non-dust storm days (green) in spring from 2013 to 2020 in northern China. Note that the O_3 positive anomaly is when the O_3 concentrations are greater than the spring average concentration from 2013 to 2020 in northern China. The stations in the black box in Fig. 2c have been selected for analysis. (For interpretation of the references to colour in this figure legend, the reader is referred to the Web version of this article.)

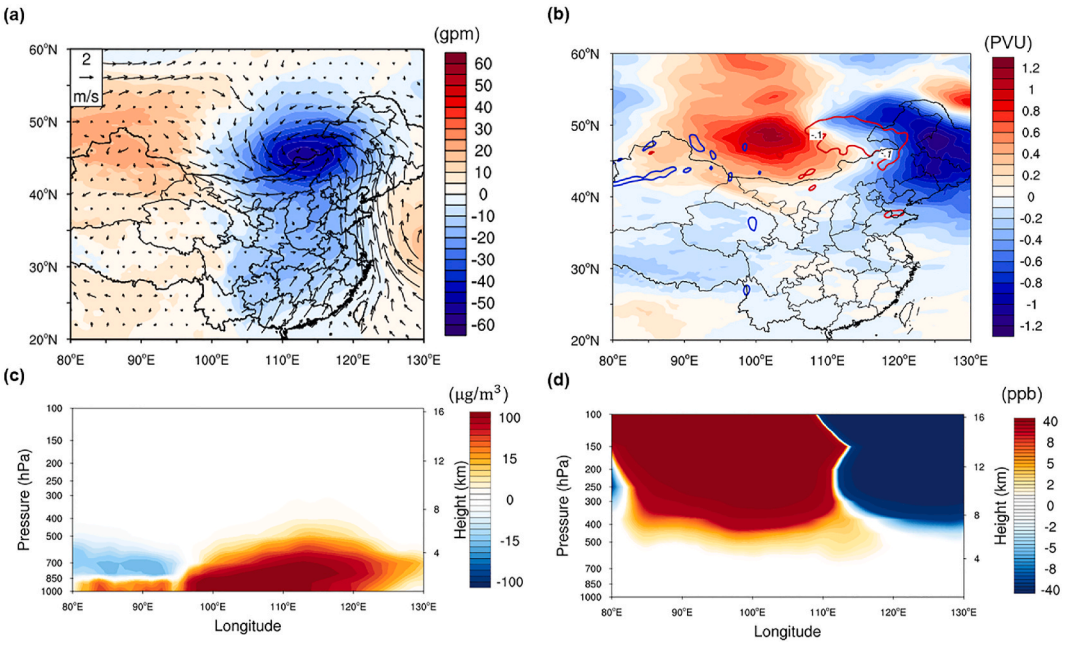

Fig. 10. (a) The spatial distribution of geopotential height and wind vectors anomalies at 925 hpa and (b) potential vorticity anomalies at 300 hPa and vertical velocity anomalies at 500 hPa (blue line encloses downward motion area while red line encloses upward motion area). And the longitude-height cross-sections (averaged range of 40°N to 50°N) of (c) dust concentrations anomalies and (d) O_3S anomalies. All anomalies are the average of the dust storms minus the spring climatology during the period from 2013 to 2020. Dust and O_3S are results of CAMS. (For interpretation of the references to colour in this figure legend, the reader is referred to the Web version of this article.)

shown in Figs. 1 and 9, the surface O_3 concentration during dust storms was higher than that during non-dust storm periods. We also compared the stratosphere-to-troposphere transport in the occurrence of positive surface O_3 anomalies during non-dust storm and dust storm in Fig. S8. There is a high PV center in north of China when positive surface O_3 anomalies occur during dust storms, yet no such signal was found during non-dust storms (Figs. S8a and S8b). In addition, compared with spring climatology, the positive surface O_3 anomaly was accompanied by a strong positive O_3S anomaly downward transport (90°E~120°E) during dust storms, while the downward transport was absent during non-dust storms (Figs. S8e and S8f). Therefore, the positive surface O_3 anomalies during dust storms are closely associated with STE. In contrast, the surface O_3 anomalies during non-dust storms are generally caused by other reasons, such as photochemical production. The ascending airflow in the east could transport the low-level air upward, which could decrease the O_3 concentration in the lower stratosphere.

4. Conclusions

In this study, combining observations and reanalysis data, the synoptic systems associated with the dust storm on March 15th, 2021 and its impact on the vertical structure of pollutants are comprehensively analyzed. The dust storm originated from Mongolia and was influenced by the Mongolian cyclone. The strong westerly airflow caused the dust outbreak and transported dust particles to northern China during the development of the Mongolian cyclone. The concentration of PM_{10} observed by air quality monitoring stations in northern China could reach 1000 μg/m^3, and the AOD captured by MODIS could reach more than 1.5. Such strong dust storms disrupted economic and social activities in numerous ways, including worsening air quality that endangered human health and reducing visibility that led to disruptions in the transportation. Under the influence of the upward motions of air related to the trough, dust particles near the surface were uplifted to the upper troposphere. At the same time, under the influence of the downward motions of air related to the trough, the dust storm event was accompanied by STE. Hence, without photochemical reaction, the average O_3 concentration near the surface in northern China reached 35 ppb in the early morning of March 15th, far beyond the average nocturnal O_3 concentration of normal days.

Furthermore, it is observed that the vertical transport of ozone and particles frequently occurs during spring dust storms in East Asia. According to the statistical results from 2013 to 2020, the occurrence of strong dust storms in northern China is usually related to the strong low-pressure system near the surface. The high winds related to the low-pressure can lead to the outbreak of dust storms and convey dust particles to the downstream regions. In addition, the upward motions of air over low-pressure systems uplift dust particles to about 400 hPa. The simultaneous downward motions of air behind low-pressure systems lead to SI, resulting in elevated surface O_3 pollution along with dust storms events. The frequency of positive surface O_3 anomalies during dust storms reach 60%. This study reveals that cyclones can play an important role in both dust storms and STE process, influencing the vertical distribution of ozone and dust particles. Considering the vital role of O_3 in atmospheric oxidation and the substantial effect of dust on both long- and short-wave radiation, such an intense vertical exchange of ozone and dust particles is expected to have a great perturbation in atmospheric chemistry and regional climate. Under the influence of global climate change, mid-latitude synoptic systems could be more active, leading to more intensive dust storms and STE processes that drastically deteriorate air quality. Therefore, early forecasting and warning systems should be further developed to mitigate impacts of such hazardous events on society.

CRediT authorship contribution statement

Yu Yang: Investigation, Visualization, Writing – original draft, preparation. **Zilin Wang:** Investigation, Writing – review & editing. **Sijia Lou:** Methodology, Validation. **Lian Xue:** Methodology, Validation. **Jinpeng Lu:** Methodology, Resources. **Hongyue Wang:** Methodology, Resources. **Jiandong Wang:** Methodology, Resources. **Aijun Ding:** Conceptualization, Supervision. **Xin Huang:** Conceptualization, Supervision.

Declaration of competing interest

The authors declare that they have no known competing financial interests or personal relationships that could have appeared to influence the work reported in this paper.

Data availability

Data will be made available on request.

Acknowledgments

This work was supported by the National Natural Science Foundation of China (41922038), the Fundamental Research Funds for the Central Universities (DLTD2107). We are grateful to the high-performance computing center of collaborative innovation center of advanced microstructures of Nanjing University for conducting anlysis and calculations in this paper.

Appendix A. Supplementary data

Supplementary data to this article can be found online at https://doi.org/10.1016/j.atmosenv.2022.119355.

References

Aili, A., Kim Oanh, N.T., 2015. Effects of dust storm on public health in desert fringe area: case study of northeast edge of Taklimakan Desert, China. Atmospheric Pollution Research 6 (5), 805–814. https://doi.org/10.5094/APR.2015.089.

Akritidis, D., Zanis, P., Pytharoulis, I., Mavrakis, A., Karacostas, Th, 2010. A deep stratospheric intrusion event down to the earth's surface of the megacity of Athens. Meteorology and Atmospheric Physics 109 (1–2), 9–18. https://doi.org/10.1007/s00703-010-0096-6.

Akritidis, Dimitris, Katragkou, E., Zanis, P., Pytharoulis, I., Melas, D., Flemming, J., et al., 2018. A deep stratosphere-to-troposphere ozone transport event over Europe simulated in CAMS global and regional forecast systems: analysis and evaluation. Atmospheric Chemistry and Physics 18 (20), 15515–15534. https://doi.org/10.5194/acp-18-15515-2018.

Akritidis, Dimitris, Pozzer, A., Flemming, J., Inness, A., Nédélec, P., Zanis, P., 2021. *A process-oriented evaluation of CAMS reanalysis ozone during tropopause folds over Europe for the period 2003–2018* (preprint). Gases/Atmospheric Modelling/Troposphere/Chemistry (chemical composition and reactions). https://doi.org/10.5194/acp-2021-998.

Alam, K., Trautmann, T., Blaschke, T., Subhan, F., 2014. Changes in aerosol optical properties due to dust storms in the Middle East and Southwest Asia. Remote Sensing of Environment 143, 216–227. https://doi.org/10.1016/j.rse.2013.12.021.

Al-Hemoud, A., Al-Sudairawi, M., Neelamanai, S., Naseeb, A., Behbehani, W., 2017. Socioeconomic effect of dust storms in Kuwait. Arabian Journal of Geosciences 10 (1), 18. https://doi.org/10.1007/s12517-016-2816-9.

AlKheder, S., AlKandari, A., 2020. The impact of dust on Kuwait International Airport operations: a case study. International Journal of Environmental Science and Technology 17 (7), 3467–3474. https://doi.org/10.1007/s13762-020-02710-3.

An, L., Che, H., Xue, M., Zhang, T., Wang, H., Wang, Y., et al., 2018. Temporal and spatial variations in sand and dust storm events in East Asia from 2007 to 2016: relationships with surface conditions and climate change. Science of The Total Environment 633, 452–462. https://doi.org/10.1016/j.scitotenv.2018.03.068.

Cao, H., Fu, C., Zhang, W., Liu, J., 2018. Characterizing sand and dust storms (SDS) intensity in China based on meteorological data. Sustainability 10 (7), 2372. https://doi.org/10.3390/su10072372.

Cariolle, D., Déqué, M., 1986. Southern hemisphere medium-scale waves and total ozone disturbances in a spectral general circulation model. Journal of Geophysical Research 91 (D10), 10825. https://doi.org/10.1029/JD091iD10p10825.

Cariolle, D., Teyssedre, H., 2007. A revised linear ozone photochemistry parameterization for use in transport and general circulation models: multi-annual simulations. Atmos. Chem. Phys. 14.

Choobari, O.A., Zawar-Reza, P., Sturman, A., 2014. The global distribution of mineral dust and its impacts on the climate system: a review. Atmospheric Research 138, 152–165. https://doi.org/10.1016/j.atmosres.2013.11.007.

Cuesta, J., Eremenko, M., Flamant, C., Dufour, G., Laurent, B., Bergametti, G., et al., 2015. Three-dimensional distribution of a major desert dust outbreak over East Asia in March 2008 derived from IASI satellite observations: 3D Distribution of Dust Plumes from IASI. Journal of Geophysical Research: Atmospheres 120 (14), 7099–7127. https://doi.org/10.1002/2014JD022406.

Cui, H., Zhao, C., Qin, Y., Zheng, X., Zheng, Y., chan, C.-Y., Chan, L.Y., 2004. An estimation of ozone flux in a stratosphere-troposphere exchange event. Chinese Science Bulletin 49 (2), 167–174. https://doi.org/10.1360/03wd0244.

Danielsen, E.F., Mohnen, V.A., 1977. Project dustorm report: ozone transport, in situ measurements, and meteorological analyses of tropopause folding. Journal of Geophysical Research 82 (37), 5867–5877. https://doi.org/10.1029/JC082i037p05867.

Ding, A., Wang, T., 2006. Influence of stratosphere-to-troposphere exchange on the seasonal cycle of surface ozone at Mount Waliguan in western China. Geophysical Research Letters 33 (3), L03803. https://doi.org/10.1029/2005GL024760.

Duce, R.A., Unni, C.K., Ray, B.J., Prospero, J.M., Merrill, J.T., 1980. Long-range atmospheric transport of soil dust from Asia to the tropical north pacific: temporal variability. Science 209 (4464), 1522–1524. https://doi.org/10.1126/science.209.4464.1522.

Eguchi, K., Uno, I., Yumimoto, K., Takemura, T., Shimizu, A., Sugimoto, N., Liu, Z., 2009. Trans-pacific dust transport: integrated analysis of NASA/CALIPSO and a global aerosol transport model. Atmospheric Chemistry and Physics 9 (9), 3137–3145. https://doi.org/10.5194/acp-9-3137-2009.

Flemming, J., Huijnen, V., Arteta, J., Bechtold, P., Beljaars, A., Blechschmidt, A.-M., et al., 2015. Tropospheric chemistry in the integrated forecasting system of ECMWF. Geoscientific Model Development 8 (4), 975–1003. https://doi.org/10.5194/gmd-8-975-2015.

Gholami, A., Khazaee, I., Eslami, S., Zandi, M., Akrami, E., 2018. Experimental investigation of dust deposition effects on photo-voltaic output performance. Solar Energy 159, 346–352. https://doi.org/10.1016/j.solener.2017.11.010.

Goudarzi, G., Daryanoosh, S.M., Godini, H., Hopke, P.K., Sicard, P., De Marco, A., et al., 2017. Health risk assessment of exposure to the Middle-Eastern Dust storms in the Iranian megacity of Kermanshah. Public Health 148, 109–116. https://doi.org/10.1016/j.puhe.2017.03.009.

Hoffmann, L., Günther, G., Li, D., Stein, O., Wu, X., Griessbach, S., et al., 2019. From ERA-Interim to ERA5: the considerable impact of ECMWF's next-generation reanalysis on Lagrangian transport simulations. Atmospheric Chemistry and Physics 19 (5), 3097–3124. https://doi.org/10.5194/acp-19-3097-2019.

Holton, J.R., Haynes, P.H., McIntyre, M.E., Douglass, A.R., Rood, R.B., Pfister, L., 1995. Stratosphere-troposphere exchange. Reviews of Geophysics 33 (4), 403–439. https://doi.org/10.1029/95RG02097.

Huang, J., Minnis, P., Chen, B., Huang, Z., Liu, Z., Zhao, Q., et al., 2008. Long-range transport and vertical structure of Asian dust from CALIPSO and surface measurements during PACDEX. Journal of Geophysical Research 113 (D23), D23212. https://doi.org/10.1029/2008JD010620.

Huang, J., Wang, T., Wang, W., Li, Z., Yan, H., 2014. Climate effects of dust aerosols over East Asian arid and semiarid regions. Journal of Geophysical Research: Atmospheres 119 (19), 11398–11416. https://doi.org/10.1002/2014JD021796.

Huang, X., Ding, A., 2021. Aerosol as a critical factor causing forecast biases of air temperature in global numerical weather prediction models. Science Bulletin 66 (18), 1917–1924. https://doi.org/10.1016/j.scib.2021.05.009.

Huang, X., Wang, Z., Ding, A., 2018. Impact of aerosol-PBL interaction on haze pollution: multiyear observational evidences in north China. Geophysical Research Letters 45 (16), 8596–8603. https://doi.org/10.1029/2018GL079239.

Huijnen, V., Miyazaki, K., Flemming, J., Inness, A., Sekiya, T., Schultz, M.G., 2020. An intercomparison of tropospheric ozone reanalysis products from CAMS, CAMS interim, TCR-1, and TCR-2. Geoscientific Model Development 13 (3), 1513–1544. https://doi.org/10.5194/gmd-13-1513-2020.

Husar, R.B., Tratt, D.M., Schichtel, B.A., Falke, S.R., Li, F., Jaffe, D., et al., 2001. Asian dust events of April 1998. Journal of Geophysical Research: Atmospheres 106 (D16), 18317–18330. https://doi.org/10.1029/2000JD900788.

In, H.-J., Park, S.-U., 2002. A simulation of long-range transport of Yellow Sand observed in April 1998 in Korea. Atmospheric Environment 36 (26), 4173–4187. https://doi.org/10.1016/S1352-2310(02)00361-8.

Indoitu, R., Orlovsky, L., Orlovsky, N., 2012. Dust storms in central Asia: spatial and temporal variations. Journal of Arid Environments 85, 62–70. https://doi.org/10.1016/j.jaridenv.2012.03.018.

Inness, A., Ades, M., Agustí-Panareda, A., Barré, J., Benedictow, A., Blechschmidt, A.-M., et al., 2019. The CAMS reanalysis of atmospheric composition. Atmospheric Chemistry and Physics 19 (6), 3515–3556. https://doi.org/10.5194/acp-19-3515-2019.

Jickells, T.D., An, Z.S., Andersen, K.K., Baker, A.R., Bergametti, G., Brooks, N., et al., 2005. Global iron connections between desert dust, ocean biogeochemistry, and climate. Science 308 (5718), 67–71. https://doi.org/10.1126/science.1105959.

Jose, S., Gharai, B., Rao, P.V.N., Dutt, C.B.S., 2016. Satellite-based shortwave aerosol radiative forcing of dust storm over the Arabian Sea: a relationship is developed between SWARF and MODIS AOD. Atmospheric Science Letters 17 (1), 43–50. https://doi.org/10.1002/asl.597.

Kaskaoutis, D.G., Kambezidis, H.D., Nastos, P.T., Kosmopoulos, P.G., 2008. Study on an intense dust storm over Greece. Atmospheric Environment 42 (29), 6884–6896. https://doi.org/10.1016/j.atmosenv.2008.05.017.

Kaufman, Y.J., Koren, I., Remer, L.A., Rosenfeld, D., Rudich, Y., 2005. The effect of smoke, dust, and pollution aerosol on shallow cloud development over the Atlantic Ocean. Proceedings of the National Academy of Sciences 102 (32), 11207–11212. https://doi.org/10.1073/pnas.0505191102.

Khaniabadi, Y.O., Daryanoosh, S.M., Amrane, A., Polosa, R., Hopke, P.K., Goudarzi, G., et al., 2017. Impact of middle eastern dust storms on human health. Atmospheric Pollution Research 8 (4), 606–613. https://doi.org/10.1016/j.apr.2016.11.005.

Kim, Y.K., Lee, H.W., Park, J.K., Moon, Y.S., 2002. The stratosphere–troposphere exchange of ozone and aerosols over Korea. Atmospheric Environment 36 (3), 449–463. https://doi.org/10.1016/S1352-2310(01)00370-3.

Knowland, K.E., Ott, L.E., Duncan, B.N., Wargan, K., 2017. Stratospheric intrusion-influenced ozone air quality exceedances investigated in the nasa MERRA-2 reanalysis: SI-influenced O_3 exceedances in MERRA-2. Geophysical Research Letters 44 (20). https://doi.org/10.1002/2017GL074532, 10,691-10,701.

Knowland, K. Emma, Doherty, R.M., Hodges, K.I., Ott, L.E., 2017. The influence of mid-latitude cyclones on European background surface ozone. Atmospheric Chemistry and Physics 17 (20), 12421–12447. https://doi.org/10.5194/acp-17-12421-2017.

Krasauskas, L., Ungermann, J., Preusse, P., Friedl-Vallon, F., Zahn, A., Ziereis, H., et al., 2021. 3-D tomographic observations of Rossby wave breaking over the North Atlantic during the WISE aircraft campaign in 2017. Atmospheric Chemistry and Physics 21 (13), 10249–10272. https://doi.org/10.5194/acp-21-10249-2021.

Kumar, K.N., Sharma, S.K., Naja, M., Phanikumar, D.V., 2020. A Rossby wave breaking-induced enhancement in the tropospheric ozone over the Central Himalayan region. Atmos. Environ. https://doi.org/10.1016/j.atmosenv.2020.117356.

Kurosaki, Y., Mikami, M., 2007. Threshold wind speed for dust emission in east Asia and its seasonal variations. Journal of Geophysical Research 112 (D17), D17202. https://doi.org/10.1029/2006JD007988.

Lee, J.-T., Son, J.-Y., Cho, Y.-S., 2007. A comparison of mortality related to urban air particles between periods with Asian dust days and without Asian dust days in Seoul, Korea, 2000–2004. Environmental Research 105 (3), 409–413. https://doi.org/10.1016/j.envres.2007.06.004.

Lefohn, A.S., Wernli, H., Shadwick, D., Limbach, S., Oltmans, S.J., Shapiro, M., 2011. The importance of stratospheric–tropospheric transport in affecting surface ozone concentrations in the western and northern tier of the United States. Atmospheric Environment 45 (28), 4845–4857. https://doi.org/10.1016/j.atmosenv.2011.06.014.

Lelieveld, J., Dentener, F.J., 2000. What controls tropospheric ozone? Journal of Geophysical Research: Atmospheres 105 (D3), 3531–3551. https://doi.org/10.1029/1999JD901011.

Li, D., Bian, J., Fan, Q., 2015. A deep stratospheric intrusion associated with an intense cut-off low event over East Asia. SCIENCE CHINA-EARTH SCIENCES 58 (1), 116–128. https://doi.org/10.1007/s11430-014-4977-2.

Li, W., Wang, W., Zhou, Y., Ma, Y., Zhang, D., Sheng, L., 2018. Occurrence and reverse transport of severe dust storms associated with synoptic weather in East Asia. Atmosphere 10 (1), 4. https://doi.org/10.3390/atmos10010004.

Liang, Q., Rodriguez, J.M., Douglass, A.R., Crawford, J.H., Olson, J.R., Apel, E., et al., 2011. Reactive nitrogen, ozone and ozone production in the Arctic troposphere and the impact of stratosphere-troposphere exchange. Atmospheric Chemistry and Physics 11 (24), 13181–13199. https://doi.org/10.5194/acp-11-13181-2011.

Lin, M., Fiore, A.M., Cooper, O.R., Horowitz, L.W., Langford, A.O., Levy, H., et al., 2012. Springtime high surface ozone events over the western United States: quantifying the role of stratospheric intrusions. Journal of Geophysical Research: Atmospheres 117, D00V22. https://doi.org/10.1029/2012JD018151.

Liu, J.-T., Jiang, X.-G., Zheng, X.-J., Kang, L., Qi, F.-Y., 2004. An intensive Mongolian cyclone genesis induced severe dust storm. Terrestrial, Atmospheric and Oceanic Sciences 15 (5), 1019–1033. https://doi.org/10.3319/TAO.2004.15.5.1019(ADSE.

Liu, L., Huang, X., Ding, A., Fu, C., 2016. Dust-induced radiative feedbacks in north China: a dust storm episode modeling study using WRF-Chem. Atmospheric Environment 129, 43–54. https://doi.org/10.1016/j.atmosenv.2016.01.019.

Liu, M., Westphal, D.L., Wang, S., Shimizu, A., Sugimoto, N., Zhou, J., Chen, Y., 2003. A high-resolution numerical study of the Asian dust storms of April 2001. Journal of Geophysical Research 108 (D23), 8653. https://doi.org/10.1029/2002JD003178.

Luo, J., Tian, W., Pu, Z., Zhang, P., Shang, L., Zhang, M., Hu, J., 2013. Characteristics of stratosphere-troposphere exchange during the Meiyu season: STRATOSPHERE-TROPOSPHERE EXCHANGE. J. Geophys. Res. Atmos. https://doi.org/10.1029/2012JD018124.

Mahowald, N.M., Baker, A.R., Bergametti, G., Brooks, N., Duce, R.A., Jickells, T.D., et al., 2005. Atmospheric global dust cycle and iron inputs to the ocean. Global Biogeochemical Cycles 19 (4), GB4025. https://doi.org/10.1029/2004GB002402.

Middleton, N., Tozer, P., Tozer, B., 2019. Sand and dust storms: underrated natural hazards. Disasters 43 (2), 390–409. https://doi.org/10.1111/disa.12320.

Miri, A., Middleton, N., 2022. Long-term impacts of dust storms on transport systems in south-eastern Iran. Natural Hazards. https://doi.org/10.1007/s11069-022-05390-z.

Miri, A., Ahmadi, H., Ekhtesasi, M.R., Panjehkeh, N., Ghanbari, A., 2009. Environmental and socio-economic impacts of dust storms in Sistan Region, Iran. International Journal of Environmental Studies 66 (3), 343–355. https://doi.org/10.1080/00207230902720170.

Mkololo, T., Mbatha, N., Sivakumar, V., Bègue, N., Coetzee, G., Labuschagne, C., 2020. Stratosphere–troposphere exchange and O3 variability in the lower stratosphere and upper troposphere over the irene SHADOZ site, South Africa. Atmosphere 11 (6), 586. https://doi.org/10.3390/atmos11060586.

Mohamed, M.I., Gehan, A.E.G., 2012. Short-term effects of dust storm on physiological performance of some wild plants in Riyadh, Saudi Arabia. African Journal of Agricultural Research 7 (47), 6305–6312. https://doi.org/10.5897/AJAR12.828.

Newell, R.E., Browell, E.V., Davis, D.D., Liu, S.C., 1997. Western Pacific tropospheric ozone and potential vorticity: implications for Asian pollution. Geophysical Research Letters 24 (22), 2733–2736. https://doi.org/10.1029/97GL02799.

Pahlavanravi, A., Miri, A., Ahmadi, H., Ekhtesasi, M.R., 2012. The Impacts of Different Kinds of Dust Storms in Hot and Dry Climate, A Case Study in Sistan Region, p. 11.

Prospero, J.M., Ginoux, P., Torres, O., Nicholson, S.E., Gill, T.E., 2002. Environmental characterization of global sources of atmospheric soil dust identified with the NIMBUS 7 Total Ozone Mapping Spectrometer (TOMS) absorbing aerosol product. Reviews of Geophysics 40 (1), 1002. https://doi.org/10.1029/2000RG000095.

Qian, W., Quan, L., Shi, S., 2002. Variations of the dust storm in China and its climatic control. Journal of Climate 15 (10), 1216–1229. https://doi.org/10.1175/1520-0442(2002)015<1216:VOTDSI>2.0.CO;2.

Ren, J.-L., Zhang, G.-L., Zhang, J., Shi, J.-H., Liu, S.-M., Li, F.-M., et al., 2011. Distribution of dissolved aluminum in the Southern Yellow Sea: influences of a dust storm and the spring bloom. Marine Chemistry 125 (1–4), 69–81. https://doi.org/10.1016/j.marchem.2011.02.004.

Salby, M.L., Callaghan, P.F., 2006. Influence of the Brewer-Dobson circulation on stratosphere-troposphere exchange. Journal of Geophysical Research 111 (D21), D21106. https://doi.org/10.1029/2006JD007051.

Seguel, R.J., Mancilla, C.A., Leiva, G.M.A., 2018. Stratospheric ozone intrusions during the passage of cold fronts over central Chile. Air Quality, Atmosphere & Health 11 (5), 535–548. https://doi.org/10.1007/s11869-018-0558-4.

Shiraiwa, M., Ueda, K., Pozzer, A., Lammel, G., Kampf, C.J., Fushimi, A., et al., 2017. Aerosol health effects from molecular to global scales. Environmental Science & Technology 51 (23), 13545–13567. https://doi.org/10.1021/acs.est.7b04417.

Škerlak, B., Sprenger, M., Wernli, H., 2014. A global climatology of stratosphere–troposphere exchange using the ERA-Interim data set from 1979 to 2011. Atmospheric Chemistry and Physics 14 (2), 913–937. https://doi.org/10.5194/acp-14-913-2014.

Sprenger, M., 2003. A northern hemispheric climatology of cross-tropopause exchange for the ERA15 time period (1979–1993). Journal of Geophysical Research 108 (D12), 8521. https://doi.org/10.1029/2002JD002636.

Stohl, A., 2003. Stratosphere-troposphere exchange: a review, and what we have learned from STACCATO. Journal of Geophysical Research 108 (D12), 8516. https://doi.org/10.1029/2002JD002490.

Su, J., Huang, J., Fu, Q., Minnis, P., Ge, J., Bi, J., 2008. Estimation of Asian dust aerosol effect on cloud radiation forcing using Fu-Liou radiative model and CERES measurements. Atmospheric Chemistry and Physics 8 (10), 2763–2771. https://doi.org/10.5194/acp-8-2763-2008.

Sun, J., Zhao, L., 2008. Numerical simulation of two East Asian dust storms in spring 2006. Earth Surface Processes and Landforms 33 (12), 1892–1911. https://doi.org/10.1002/esp.1734.

Takemi, T., 2005. Dust storms and cyclone tracks over the arid regions in east Asia in spring. Journal of Geophysical Research 110 (D18), D18S11. https://doi.org/10.1029/2004JD004698.

Takemura, T., Uno, I., Nakajima, T., Higurashi, A., Sano, I., 2002. Modeling study of long-range transport of Asian dust and anthropogenic aerosols from East Asia. Geophysical Research Letters 29 (24), 2158. https://doi.org/10.1029/2002GL016251.

Tan, S.-C., Shi, G.-Y., Wang, H., 2012. Long-range transport of spring dust storms in Inner Mongolia and impact on the China seas. Atmospheric Environment 46, 299–308. https://doi.org/10.1016/j.atmosenv.2011.09.058.

Tan, S.-C., Li, J., Che, H., Chen, B., Wang, H., 2017. Transport of East Asian dust storms to the marginal seas of China and the southern North Pacific in spring 2010. Atmospheric Environment 148, 316–328. https://doi.org/10.1016/j.atmosenv.2016.10.054.

Textor, C., Schulz, M., Guibert, S., Kinne, S., Balkanski, Y., Bauer, S., et al., 2006. Analysis and quantification of the diversities of aerosol life cycles within AeroCom. Atmospheric Chemistry and Physics 6 (7), 1777–1813. https://doi.org/10.5194/acp-6-1777-2006.

Tsai, F., Chen, G.T.-J., Liu, T.-H., Lin, W.-D., Tu, J.-Y., 2008. Characterizing the transport pathways of Asian dust. Journal of Geophysical Research 113 (D17), D17311. https://doi.org/10.1029/2007JD009674.

Wang, F., Yang, T., Wang, Z., Cao, J., Liu, B., Liu, J., et al., 2021. A comparison of the different stages of dust events over Beijing in March 2021: the effects of the vertical structure on near-surface particle concentration. Remote Sensing 13 (18), 3580. https://doi.org/10.3390/rs13183580.

Wang, H., Wang, W., Huang, X., Ding, A., 2020. Impacts of stratosphere-to-troposphere-transport on summertime surface ozone over eastern China. Science Bulletin 65 (4), 276–279. https://doi.org/10.1016/j.scib.2019.11.017.

Wang, S., Wang, J., Zhou, Z., Shang, K., 2005. Regional characteristics of three kinds of dust storm events in China. Atmospheric Environment 39 (3), 509–520. https://doi.org/10.1016/j.atmosenv.2004.09.033.

Wang, W., Huang, J., Zhou, T., Bi, J., Lin, L., Chen, Y., et al., 2013. Estimation of radiative effect of a heavy dust storm over northwest China using Fu–Liou model and ground measurements. Journal of Quantitative Spectroscopy and Radiative Transfer 122, 114–126. https://doi.org/10.1016/j.jqsrt.2012.10.018.

Wang, Y., Wang, H., Wang, W., 2020. A stratospheric intrusion-influenced ozone pollution episode associated with an intense horizontal-trough event. Atmosphere 11 (2), 164. https://doi.org/10.3390/atmos11020164.

Wang, Z., Huang, X., Ding, A., 2018. Dome effect of black carbon and its key influencing factors: a one-dimensional modelling study. Atmospheric Chemistry and Physics 18 (4), 2821–2834. https://doi.org/10.5194/acp-18-2821-2018.

Wang, Z., Huang, X., Wang, N., Xu, J., Ding, A., 2020. Aerosol-radiation interactions of dust storm deteriorate particle and ozone pollution in East China. Journal of Geophysical Research: Atmospheres 125 (24). https://doi.org/10.1029/2020JD033601.

Wei, W., Pi, D., Yan, D., Xiao, L., Zhang, W., Chen, T., et al., 2018. Study on a typical dust pollution process in North China in spring in 2017. Acta Scientiae Circumstantiae 38 (5), 1699–1707.

Yang, S., Wang, Z., Huang, X., Wang, W., Sheng, L., Zhou, Y., 2021. Meteorological feedback and eco-environmental impact of Asian dust: a simulation study. Atmospheric Environment 253, 118350. https://doi.org/10.1016/j.atmosenv.2021.118350.

Yin, Z., Wan, Y., Zhang, Y., Wang, H., 2021. Why super sandstorm 2021 in North China? National Science Review. https://doi.org/10.1093/nsr/nwab165 nwab165.

Young, P.J., Archibald, A.T., Bowman, K.W., Lamarque, J.-F., Naik, V., Stevenson, D.S., et al., 2013. Pre-industrial to end 21st century projections of tropospheric ozone from the atmospheric chemistry and climate model intercomparison project (ACCMIP). Atmospheric Chemistry and Physics 13 (4), 2063–2090. https://doi.org/10.5194/acp-13-2063-2013.

Zender, C.S., Miller, R.L.R.L., Tegen, I., 2004. Quantifying mineral dust mass budgets: Terminology, constraints, and current estimates. Eos, Transactions American Geophysical Union 85 (48), 509–512. https://doi.org/10.1029/2004EO480002.

Zhang, X.Y., Gong, S.L., Zhao, T.L., Arimoto, R., Wang, Y.Q., Zhou, Z.J., 2003. Sources of Asian dust and role of climate change versus desertification in Asian dust emission. Geophysical Research Letters 30 (24), 2272. https://doi.org/10.1029/2003GL018206.

Zhao, Linna, Zhao, S., 2006. Diagnosis and simulation of a rapidly developing cyclone related to a severe dust storm in East Asia. Global and Planetary Change 52 (1–4), 105–120. https://doi.org/10.1016/j.gloplacha.2006.02.003.

Zhang, J., Li, D., Bian, J., Bai, Z., 2021. Deep stratospheric intrusion and Russian wildfire induce enhanced tropospheric ozone pollution over the northern Tibetan Plateau. Atmos. Res. https://doi.org/10.1016/j.atmosres.2021.105662.

Zhao, Liying, Wang, W., Hao, T., Qu, W., Sheng, L., Luo, C., et al., 2020. The autumn haze-fog episode enhanced by the transport of dust aerosols in the Tianjin area. Atmospheric Environment 237, 117669. https://doi.org/10.1016/j.atmosenv.2020.117669.

Zhu, A., Ramanathan, V., Li, F., Kim, D., 2007. Dust plumes over the Pacific, Indian, and Atlantic oceans: climatology and radiative impact. Journal of Geophysical Research 112, D16208. https://doi.org/10.1029/2007JD008427.